

Dimolybdenum complexes containing bridging acetate ligands and anions of *N,N'*-di(2-methoxyphenyl)formamidine

Ying-Yann Wu^a, Jhy-Der Chen^{a,*}, Lin-Shu Liou^b, Ju-Chun Wang^b

^a Department of Chemistry, Chung-Yuan Christian University, Chung-Li, Taiwan, ROC

^b Department of Chemistry, Soochow University, Taipei, Taiwan, ROC

Received 20 December 2001; accepted 13 February 2002

Abstract

The syntheses, structures and NMR spectra of quadruply bonded complexes containing three, two or one bridging acetate ligands and anions of *N,N'*-di(2-methoxyphenyl)formamidine (*o*-HDMophF), of the types Mo₂(O₂CCH₃)₃(*o*-DMophF) (**1**), *trans*-Mo₂(O₂CR)₂(*o*-DMophF)₂ (R = CH₃, **2**; CF₃, **3**; Prⁿ, **4**) and Mo₂(O₂CCH₃)(*o*-DMophF)Cl₂(PMe₃)₂ (**5**), are discussed. Complex **1** was prepared by reaction of Mo₂(O₂CCH₃)₄ with excess *o*-HDMophF in THF. The reactions of Mo₂(O₂CCH₃)₄ and Mo₂(O₂CPrⁿ)₄ with excess lithiated formamidine afforded complexes **2** and **4**, respectively. Complex **3** was prepared by reaction of Mo₂(O₂CCF₃)₄ with *o*-HDMophF in THF and complex **5** was prepared by reaction of **1** with (CH₃)₃SiCl and PMe₃ in THF/CH₂Cl₂. Their UV–Vis and NMR spectra have been recorded and their structures have been determined by X-ray crystallography. The *o*-DMophF[−] ligands show two different conformations, *s-trans,s-trans* and *s-cis,s-trans*, in compounds **1**–**5**. The study on ³¹P{¹H} NMR spectrum of **5** concluded that the through metal–metal quadruple bonding coupling [³J_{P–Mo–Mo–P}] is about 16 ± 1 Hz. The position of the monodentate phosphine ligand, i.e. *cis* or *trans* to the acetate or similar ligands, can be determined by evaluating the [³J_{C–P}] coupling constant. © 2002 Elsevier Science B.V. All rights reserved.

Keywords: Dimolybdenum complexes; Bridging acetate; Formamidine; ³¹P NMR

1. Introduction

The coordination chemistry of formamidinate compounds has been investigated extensively during recent years [1–5]. Many efforts have been concentrated in their ability to form bridges between metal atoms. Preparations, structures and spectroscopic properties of tetrakis(μ-diarylformamidinato)dimolybdenum complexes of the type Mo₂(form)₄, where form is the generic formamidine, were the subjects of several studies [6]. Crystalline Mo₂(form)₄ can be prepared by stoichiometric ligand metathesis between the dimolybdenum tetraacetate Mo₂(O₂CR)₄ and the lithiated formamidine. To our knowledge, no mixed formamidinate–acetate dimolybdenum species, which can be envisaged as the intermediates of the stepwise decarboxylation of

Mo₂(O₂CR)₄ to form Mo₂(form)₄, has been reported. The only dimolybdenum analogues reported are the acetamidinate compound *trans*-Mo₂(O₂CCH₃)₂(DXylA)₂(THF)₂ [7a], and the benzamidinate compounds *trans*-Mo₂(O₂CCH₃)₂[μ-*N,N'*-PhC(NSiMe₃)₂]₂ [7b] and *trans*-Mo₂(O₂CPh)₂[μ-*N,N'*-PhC(NSiMe₃)₂]₂ [7c]. Some square and triangular arrays of Mo₂⁴⁺ units that are bridged by formamidinate and dicarboxylate ligands have also been reported [7d]. We report here the first mixed formamidinate–acetate complexes of the dinuclear types Mo₂(O₂CCH₃)₃(*o*-DMophF), *trans*-Mo₂(O₂CR)₂(*o*-DMophF)₂ (R = CH₃, CF₃ and Prⁿ) and Mo₂(O₂CCH₃)(*o*-DMophF)Cl₂(PMe₃)₂, which contain three, two or one bridging acetate ligands and anions of *N,N'*-di(2-methoxyphenyl)formamidine (*o*-HDMophF). The syntheses, structures and NMR spectra of these complexes form the subject of this report.

* Corresponding author. Fax: +886-3-456 310

2. Experimental

2.1. General procedures

All manipulations were carried out under dry, oxygen-free nitrogen by using Schlenk techniques, unless otherwise noted. Solvents were dried and deoxygenated by refluxing over the appropriate reagents before use. Hexanes, THF and ether were purified by distillation from sodium–benzophenone, acetonitrile from CaH₂ and dichloromethane from P₂O₅. The visible absorption spectra were recorded on a Hitachi U-2000 spectrophotometer. NMR spectra were measured on a Bruker Avance 300 MHz spectrometer. 85% H₃PO₄ and CFC₃ were used as standards for ³¹P{¹H} and ¹⁹F{¹H} NMR, respectively. IR spectra were obtained from a JASCO FT/IR-460 plus spectrometer. Elemental analyses were obtained from a PE 2400 series II CHNS/O analyzer.

2.2. Starting material

The complexes Mo₂(O₂CCH₃)₄ [8], Mo₂(O₂CCF₃)₄ [9], Mo₂(O₂CPrⁿ)₄ [10] and the ligand *N,N'*-di(2-methoxyphenyl)formamidine (*o*-HDMophF) were prepared according to previously reported procedures [11].

2.3. Preparation of Mo₂(O₂CCH₃)₃(*o*-HDMophF)

Mo₂(O₂CCH₃)₄ (1.0 g, 2.34 mmol) and *o*-HDMophF (1.8 g, 7.02 mmol) was placed in a flask containing 15 ml THF. The mixture was then refluxed for 2 days to yield a brown solution and a yellow solid. The solid was filtered, washed by ether and then dissolved in 10 ml CH₂Cl₂ to give a yellow solution. The solvent was removed under vacuum to leave the yellow product. Yield: 0.70 g (48%). UV–Vis: 448 nm (CH₂Cl₂, ε = 1966 M⁻¹ cm⁻¹). ¹H NMR (CDCl₃, ppm): 9.58 (s, 1H, CH), 7.55 (d, 2H, H^{ortho}), 6.97 (t, 2H, H^{meta}), 6.99 (t, 2H, H^{para}), 6.68 (d, 2H, H^{meta}), 3.26 (s, 6H, OCH₃), 2.77 (s, 3H, CH₃^{trans}), 2.58 (s, 6H, CH₃^{cis}). ¹³C NMR (CDCl₃, ppm): 181.34, 152.74, 149.10, 138.11, 123.57, 121.90, 115.95, 112.02, 56.05, 23.60. Calc. for C₂₁H₂₄Mo₂N₂O₈ (MW 624.30): C, 40.40; H, 3.87; N, 4.49. Found: C, 40.44; H, 3.57; N, 4.66%. IR (KBr disk): 1658(m), 1585(m), 1537(s), 1425(s), 1336(s), 1242(s), 1171(m), 1119(s), 1016(s), 748(m), 673(m).

2.4. Preparation of trans-Mo₂(O₂CCH₃)₂(*o*-HDMophF)₂

o-HDMophF (1.8 g, 7.02 mmol) was placed in a flask containing 10 ml THF. *n*-BuLi (4.4 ml, 1.6 M per hexane) was then added. The mixture was stirred at 0 °C for 30 min to yield an orange solution. Mo₂(OAc)₄ (1.0 g, 2.34 mmol) was then added and the mixture refluxed for another 20 h. The solid was filtered, washed

by ether and then dried under reduced pressure to give the yellow product. Yield: 1.31 g (68%). UV–Vis: 459 nm (CH₂Cl₂, ε = 1617 M⁻¹ cm⁻¹). ¹H NMR (CDCl₃, ppm): 8.99 (s, 2H, CH), 7.26 (d, 4H, H^{ortho}), 6.88 (t, 4H, H^{meta}), 6.92 (t, 4H, H^{para}), 6.69 (d, 4H, H^{meta}), 3.15 (s, 12H, OCH₃), 2.53 (s, 6H, CH₃). ¹³C NMR (CDCl₃, ppm): 179.50, 156.72, 150.94, 139.50, 123.42, 121.39, 120.35, 112.13, 55.71, 23.87. Calc. for C₃₄H₃₆Mo₂N₄O₈ (MW 820.56): C, 49.77; H, 4.42; N, 6.83. Found: C, 49.37; H, 4.37; N, 6.45%. IR (KBr disk): 1560(m), 1493(s), 1420(m), 1323(m), 1247(m), 1206(s), 1178(s), 1052(s), 1060(m), 745(m), 669(m), 625(s), 437(m).

2.5. Preparation of trans-Mo₂(O₂CCF₃)₂(*o*-HDMophF)₂

Mo₂(O₂CCF₃)₄ (1.0 g, 1.55 mmol) and *o*-HDMophF (1.2 g, 4.66 mmol) was placed in a flask containing 10 ml CH₂Cl₂. The mixture was then stirred at room temperature (r.t.) for 20 h to yield a yellow solution and a yellow solid. The solid was filtered, washed by ether and then dried under reduced pressure to give the yellow product. Yield: 1.23 g (85%). UV–Vis: 445 nm (CH₂Cl₂, ε = 855 M⁻¹ cm⁻¹). ¹H NMR (CDCl₃, ppm): 9.18 (s, 2H, CH), 7.33 (d, 4H, H^{ortho}), 6.95 (t, 4H, H^{meta}), 6.99 (t, 4H, H^{para}), 6.70 (d, 4H, H^{meta}), 3.09 (s, 12H, OCH₃). ¹³C NMR (CDCl₃, ppm): 160.94 (q, ²J_{C-F} = 39.10 Hz), 158.10, 150.77, 138.50, 127.80, 121.50, 119.97, 113.37 (q, ¹J_{C-F} = 283.65 Hz), 111.72, 55.38. ¹⁹F{¹H} NMR (CDCl₃, ppm): -72.30 (¹J_{C-F} = 283.25 Hz, ²J_{C-F} = 38.84 Hz). Calc. for C₃₄H₃₀F₆Mo₂N₄O₈ (MW 928.50): C, 43.98; H, 3.26; N, 6.03. Found: C, 43.39; H, 3.47; N, 6.34%. IR (KBr disk): 1609(m), 1534(m), 1502(m), 1465(s), 1350(s), 1330(m), 1237(s), 1212(s), 1196(m), 1172(s), 1144(m), 1120(m), 1044(s), 1059(s), 1012(m), 936(s), 755(s), 745(m), 728(m), 492(s), 444(s).

2.6. Preparation of trans-Mo₂(O₂CPrⁿ)₂(*o*-HDMophF)₂

o-HDMophF (0.71 g, 2.77 mmol) was placed in a flask containing 10 ml THF. *n*-BuLi (1.7 ml, 1.6 M per hexane) was then added. The mixture was stirred at 0 °C for 30 min to yield an orange solution. Mo₂(O₂CPrⁿ)₄ (0.5 g, 0.93 mmol) was then added and the mixture refluxed for another 20 h. The solid was filtered, washed by ether and then dried under reduced pressure to give the yellow product. Yield: 0.71 g (87%). UV–Vis: 460 nm (CH₂Cl₂, ε = 2415 M⁻¹ cm⁻¹). ¹H NMR (CD₂Cl₂, ppm): 8.99 (s, 2H, CH), 7.25 (d, 4H, H^{ortho}), 6.92 (t, 4H, H^{meta}), 6.96 (t, 4H, H^{para}), 6.73 (d, 4H, H^{meta}), 3.16 (s, 12H, OCH₃), 2.79 (t, 4H, CH₂), 1.78 (q, 4H, CH₂), 0.95 (t, 6H, CH₃). ¹³C NMR (CD₂Cl₂, ppm): 182.80, 156.80, 151.05, 139.56, 123.75, 121.62, 120.48, 112.21, 55.78, 39.30, 20.68, 13.75. Calc. for C₃₈H₄₄Mo₂N₄O₈ (MW 876.56): C, 52.06; H, 5.06; N, 6.39. Found: C, 51.96; H, 4.76; N, 6.29%. IR (KBr disk): 2964(m), 1581(s), 1558(m), 1536(s), 1492(s), 1446(s),

Table 1
Crystal data for compounds 1–5

Compound	1	2·2CH ₂ Cl ₂	3	4	5
Formula	C ₂₁ H ₂₄ Mo ₂ N ₂ O ₈	C ₃₆ H ₄₀ Cl ₄ Mo ₂ N ₄ O ₈	C ₃₄ H ₃₀ F ₆ Mo ₂ N ₄ O ₈	C ₃₈ H ₄₄ Mo ₂ N ₄ O ₈	C ₂₃ H ₃₆ Cl ₂ Mo ₂ N ₂ O ₄ P ₂
Formula weight	624.30	990.40	928.50	876.65	729.26
Crystal system	monoclinic	monoclinic	triclinic	triclinic	triclinic
Space group	<i>P</i> 2 ₁ / <i>c</i>	<i>P</i> 2 ₁	<i>P</i> $\bar{1}$	<i>P</i> $\bar{1}$	<i>P</i> $\bar{1}$
<i>a</i> (Å)	9.816(1)	12.910(2)	9.069(8)	8.546(1)	9.836(1)
<i>b</i> (Å)	20.784(1)	8.506(2)	9.712(9)	9.785(1)	10.941(1)
<i>c</i> (Å)	11.781(1)	19.699(4)	12.165(11)	12.266(1)	16.069(2)
α (°)	90	90	72.345(8)	77.678(6)	102.186(7)
β (°)	97.453(1)	105.383(2)	76.084(7)	80.516(5)	105.421(6)
γ (°)	90	90	66.923(7)	67.038(6)	103.016(8)
<i>V</i> (Å ³)	2383.2(2)	2085.8(6)	930(2)	918.91(13)	1555.0(3)
<i>Z</i>	4	2	1	1	2
<i>D</i> _{calc} (g cm ⁻³)	1.740	1.577	1.658	1.584	1.558
<i>F</i> (000)	1248	1000	464	448	736
Crystal size (mm)	0.4 × 0.6 × 0.6	0.35 × 0.4 × 0.5	0.12 × 0.6 × 0.85	0.1 × 0.1 × 0.2	0.1 × 0.1 × 0.4
μ (Mo K α) (mm ⁻¹)	1.100	0.910	0.759	0.740	1.110
Data collection instrument	Siemens CCD	Siemens CCD	Siemens CCD	Bruker AXS	Bruker AXS
Radiation monochromated in incident beam (λ (Mo K α) (Å))	0.71073	0.71073	0.71073	0.71073	0.71073
Range (2 θ) for data collection (°)	4.00 ≤ 2 θ ≤ 50.04	4.28 ≤ 2 θ ≤ 49.92	4.68 ≤ 2 θ ≤ 49.80	4.58 ≤ 2 θ ≤ 50.00	4.00 ≤ 2 θ ≤ 50.00
Temperature (°C)	25	25	25	25	25
Limiting indices	−11 ≤ <i>h</i> ≤ 11, −24 ≤ <i>k</i> ≤ 17, −13 ≤ <i>l</i> ≤ 14	−15 ≤ <i>h</i> ≤ 15, −10 ≤ <i>k</i> ≤ 4, −13 ≤ <i>l</i> ≤ 23	−5 ≤ <i>h</i> ≤ 10, −11 ≤ <i>k</i> ≤ 11, −10 ≤ <i>l</i> ≤ 14	−1 ≤ <i>h</i> ≤ 10, −10 ≤ <i>k</i> ≤ 11, −14 ≤ <i>l</i> ≤ 14	−1 ≤ <i>h</i> ≤ 11, −12 ≤ <i>k</i> ≤ 12, −19 ≤ <i>l</i> ≤ 18
Reflections collected	11 776	6477	3914	3915	6456
Independent reflections	4180 [<i>R</i> _{int} = 0.0319]	4604 [<i>R</i> _{int} = 0.0296]	2835 [<i>R</i> _{int} = 0.0421]	3214, [<i>R</i> _{int} = 0.0657]	5420, [<i>R</i> _{int} = 0.0278]
Refinement method	Full-matrix least-squares on <i>F</i> ²	Full-matrix least-squares on <i>F</i> ²	Full-matrix least-squares on <i>F</i> ²	Full-matrix least-squares on <i>F</i> ²	Full-matrix least-squares on <i>F</i> ²
Data/restraints/parameters	4180/0/394	4604/1/464	2835/0/304	3214/0/323	5420/0/430
Quality-of-fit indicator ^c	1.153	1.065	1.160	1.049	1.031
Final <i>R</i> indices [<i>I</i> > 2 σ (<i>I</i>)] ^{a,b}	<i>R</i> ₁ = 0.0265, <i>wR</i> ₂ = 0.0682	<i>R</i> ₁ = 0.0489, <i>wR</i> ₂ = 0.1225	<i>R</i> ₁ = 0.0521, <i>wR</i> ₂ = 0.1181	<i>R</i> ₁ = 0.0341, <i>wR</i> ₂ = 0.0701	<i>R</i> ₁ = 0.0414, <i>wR</i> ₂ = 0.0862
<i>R</i> indices (all data)	<i>R</i> ₁ = 0.0279, <i>wR</i> ₂ = 0.0694	<i>R</i> ₁ = 0.0515, <i>wR</i> ₂ = 0.1265	<i>R</i> ₁ = 0.0609, <i>wR</i> ₂ = 0.1298	<i>R</i> ₁ = 0.0538, <i>wR</i> ₂ = 0.0759	<i>R</i> ₁ = 0.0677, <i>wR</i> ₂ = 0.0983
Largest difference peak and hole (e Å ⁻³)	0.274 and −0.712	1.052 and −0.931	1.295 and −1.118	0.456 and −1.079	1.022 and −0.596

^a $R_1 = \sum ||F_o| - |F_c|| / \sum |F_o|$.

^b $wR_2 = [\sum w(F_o^2 - F_c^2)^2 / \sum w(F_o^2)^2]^{1/2}$, $w = 1/[\sigma^2(F_o^2) + (ap)^2 + (bp)]$, $P = [\max(F_o^2 - 0) + 2(F_c^2)]/3$, $a = 0.0342$, $b = 1.3641$ (1); $a = 0.0588$, $b = 6.6239$ (2); $a = 0.0333$, $b = 5.3917$ (3); $a = 0.0295$, $b = 0.4070$ (4); $a = 0.0369$, $b = 2.0448$ (5).

^c Quality-of-fit = $[\sum w(|F_o^2| - |F_c^2|)^2 / (N_{\text{observed}} - N_{\text{parameters}})]^{1/2}$.

1410(m), 1242(s), 1209(m), 1174(m), 1116(m), 1047(w), 1012(m), 744(m), 642(m), 526(w), 443(w).

2.7. Preparations of Mo₂(O₂CCH₃)₂(*o*-DMophF)Cl₂(PMe₃)₂

Mo₂(O₂CCH₃)₂(*o*-DMophF)₂ (0.41 g, 0.50 mmol) was placed in a flask containing 5 ml THF and 5 ml CH₂Cl₂, followed by addition of Me₃SiCl (0.38 ml, 3.0 mmol). The mixture was stirred at r.t. for 1 h to yield a brown solution. PMe₃ (1 ml, 1 M per THF) was then

added and the mixture refluxed for another 16 h. The solvent was removed under vacuum to leave a purple red solid. The solid was washed by ether and then dried under reduced pressure. Yield: 0.12 g (32%). UV–Vis: 531 nm (CH₂Cl₂, $\epsilon = 1334 \text{ M}^{-1} \text{ cm}^{-1}$). ¹H NMR (CDCl₃, ppm): 9.52 (d, 1H, CH, ⁴*J*_{H–P} = 4.09 Hz), 7.67 (d, 1H, H^{ortho}), 7.38 (d, 1H, H^{ortho}), 7.01 (t, 1H, H^{meta}), 6.99 (t, 1H, H^{meta}), 6.94 (t, 1H, H^{para}), 6.97 (t, 1H, H^{para}), 6.61 (d, 1H, H^{meta}), 6.73 (d, 1H, H^{meta}), 3.23 (s, 3H, OCH₃), 3.40 (s, 3H, OCH₃), 1.57 (d, 9H, PMe₃, ²*J*_{H–P} = 8.38 Hz), 1.21 (d, 9H, PMe₃, ²*J*_{H–P} = 8.50 Hz).

^{13}C NMR (CDCl_3 , ppm): 182.38 (d, $^3J_{\text{C-P}} = 3.5$ Hz), 156.30 (d, $^3J_{\text{C-P}} = 2.2$ Hz), 150.68, 148.25, 139.34 (d, $^3J_{\text{C-P}} = 2.1$ Hz), 137.36, 124.79, 123.84, 121.61, 121.31, 120.38, 115.48, 112.37, 111.24, 55.88, 54.15, 23.69, 12.42 (d, $^1J_{\text{C-P}} = 13.4$ Hz), 12.11 (d, $^1J_{\text{C-P}} = 11.6$ Hz). $^{31}\text{P}\{^1\text{H}\}$ NMR (CDCl_3 , ppm): -3.58 (d, $^3J_{\text{P-P}} = 15.2$ Hz), -8.37 (d, $^3J_{\text{P-P}} = 15.2$ Hz). Calc. for $\text{C}_{23}\text{H}_{36}\text{Cl}_2\text{Mo}_2\text{N}_2\text{O}_4\text{P}_2$ (MW 729.26): C, 37.88; H, 4.97; N, 3.84. Found: C, 37.66; H, 4.84; N, 3.89%. IR (KBr disk): 2964(m), 2906(m), 2835(w), 1685(s), 1535(m), 1500(m), 1460(w), 1427(w), 1261(s), 1115(s), 1020(s), 953(m), 802(s), 750(m), 675(w), 488(w).

3. X-ray crystallography

The diffraction data of **1–5** were collected on a Siemens CCD or Bruker AXS diffractometer, which was equipped with a graphite-monochromated Mo $K\alpha$ ($\lambda_\alpha = 0.71073$ Å) radiation. Data reduction was carried by standard methods with use of well-established computational procedures [12]. A colorless crystal of **1** was mounted on the top of a glass fiber with epoxy cement. The hemisphere data collection method was used to scan the data points at $4.00 < 2\theta < 50.04^\circ$. The structure factors were obtained after Lorentz and polarization corrections. The positions of some of the heavier atoms were located by the direct method. The remaining atoms were found in a series of alternating difference Fourier maps and least-square refinements. The final residuals of the refinement were $R_1 = 0.0265$ and $wR_2 = 0.0682$. The X-ray crystallographic procedures for **2–5** were similar to those for **1**. Basic information pertaining to crystal parameters and structure refinement is summarized in Table 1.

4. Results and discussion

4.1. Synthesis and structures

The yellow complex $\text{Mo}_2(\text{O}_2\text{CCH}_3)_3(o\text{-DMophF})$ (**1**) was prepared by reaction of $\text{Mo}_2(\text{O}_2\text{CCH}_3)_4$ with excess $o\text{-HDMophF}$ in THF. The reactions of lithiated formamidine with $\text{Mo}_2(\text{O}_2\text{CCH}_3)_4$, $\text{Mo}_2(\text{O}_2\text{CCF}_3)_4$ and $\text{Mo}_2(\text{O}_2\text{CPr}^n)_4$ afforded the complexes $trans\text{-Mo}_2(\text{O}_2\text{CCH}_3)_2(o\text{-DMophF})_2$ (**2**), $trans\text{-Mo}_2(\text{O}_2\text{CCF}_3)_2(o\text{-DMophF})_2$ (**3**), and $trans\text{-Mo}_2(\text{O}_2\text{CPr}^n)_2(o\text{-DMophF})_2$ (**4**), respectively. The reaction of **2** with $(\text{CH}_3)_3\text{SiCl}$ and PMe_3 in THF gave the complex $\text{Mo}_2(\text{O}_2\text{CCH}_3)(o\text{-DMophF})\text{Cl}_2(\text{PMe}_3)_2$ (**5**). Their structures have been determined by spectroscopic methods and by X-ray crystallography. Although the tetrakis($\mu\text{-}N,N'$ -di(2-methoxyphenyl)formamidine) dichromium complex [13] has been reported, attempts to prepare the dimolybdenum analogue were not successful. It is noted that

o -demethylation reaction has been found in the reaction between $\text{Ru}_2(\text{OAc})_4\text{Cl}$ and $o\text{-DMophF}$, which was attributed to the electron deficiency at the Ru_2 center (formal oxidation state = 5+) [14].

Yellow crystals of **1** conform to the space group $P2_1/c$ with four molecules in a unit cell. Fig. 1 shows the ORTEP diagram for **1**. Selected bond distances and angles are listed in Table 2. The molecular structure of **1** consists of two molybdenum atoms [$\text{Mo}\text{--}\text{Mo} = 2.0933$ (3) Å] which are spanned by three bridging acetate ligand and one $o\text{-DMophF}^-$ ligand. The $o\text{-DMophF}^-$ ligand coordinates to the molybdenum centers through the two central nitrogen atoms and is arranged in a $s\text{-trans},s\text{-trans}$ conformation, following the conformational descriptor for di(m -aloxylphenyl)formamidine proposed by Ren and co-authors [15]. Such conformation results in two short $\text{Mo}\cdots\text{O}$ distances. Complex **1** is of significance, because, it is the first dimolybdenum paddlewheel species which contains three acetate ligands and one formamidinate ligand, although dimolybdenum complex containing three acetate and other ligands, such as $[\text{Mo}_2(\text{O}_2\text{CCH}_3)_3(\text{S}_2\text{CPEt}_3)]\text{BF}_4$ [16], and $\text{Mo}_2(\text{O}_2\text{CCH}_3)_3(\text{BAII})$ (BAII = bis(arylimino)isoindoline) [17] are known.

Yellow crystals of **2**· $2\text{CH}_2\text{Cl}_2$ conform to the space group $P2_1$ with two molecules in a unit cell. Yellow crystals of both complexes **3** and **4** conform to the space group $P\bar{1}$ with one molecule in a unit cell. Figs. 2–4 show the ORTEP diagram for **2–4**, respectively. Selected bond distances and angles for **2–4** are listed in Table 2. The molecular structures of **2–4** consists of two molybdenum atoms [$\text{Mo}\text{--}\text{Mo} = 2.108$ (1) for **2**, 2.133 (2) for **3** and 2.1088 (6) Å for **4**] which are spanned by two $trans$ bridging acetate ligands and two $trans$ bridging $o\text{-DMophF}^-$ ligands. This $trans$ configuration

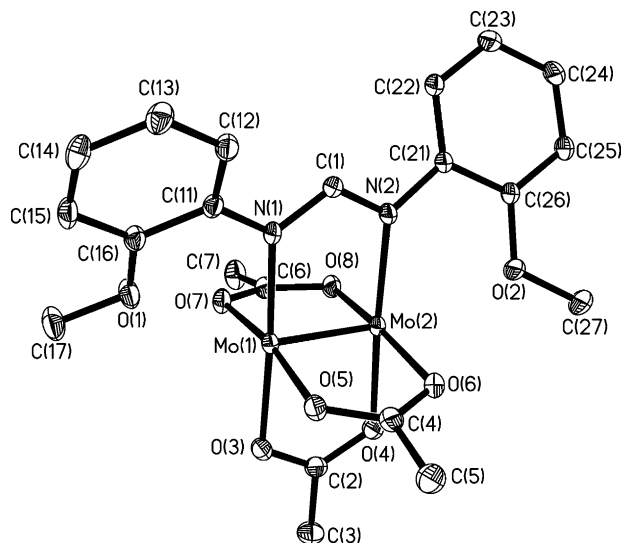


Fig. 1. ORTEP drawing for complex **1**. Thermal ellipsoids shown at 50% probability level.

Table 2
Selected bond distances (Å) and angles (°) for 1–4

1	2	3	4				
<i>Bond distances</i>							
Mo(1)–Mo(2)	2.0933(3)	Mo(1)–Mo(2)	2.108(1)	Mo–Mo(A)	2.133(2)	Mo–Mo(A)	2.1088(6)
Mo(1)–O(5)	2.109(2)	Mo(1)–N(3)	2.116(7)	Mo–N(2A)	2.134(5)	Mo–N(2A)	2.130(3)
Mo(1)–O(7)	2.135(2)	Mo(1)–O(7)	2.127(7)	Mo–O(4A)	2.138(4)	Mo–O(4A)	2.123(2)
Mo(1)–O(3)	2.139(2)	Mo(1)–O(5)	2.141(8)	Mo–O(3)	2.154(5)	Mo–O(3)	2.124(2)
Mo(1)–N(1)	2.144(2)	Mo(1)–N(1)	2.165(7)	Mo–N(1)	2.171(5)	Mo–N(1)	2.177(3)
Mo(2)–O(8)	2.114(2)	Mo(2)–O(8)	2.112(7)	Mo(A)–O(4)	2.138(4)	Mo(A)–O(4)	2.123(2)
Mo(2)–O(6)	2.125(2)	Mo(2)–O(6)	2.144(7)	Mo(A)–N(2)	2.134(5)	Mo(A)–N(2)	2.130(3)
Mo(2)–O(4)	2.129(2)	Mo(2)–N(2)	2.148(7)	Mo–O(1)	2.576(5)	Mo–O(1)	2.602(2)
Mo(2)–N(2)	2.136(2)	Mo(2)–N(4)	2.201(7)				
Mo(1)···O(1)	2.681(2)	Mo(1)···O(1)	2.600(7)				
Mo(2)···O(2)	2.667(2)	Mo(2)···O(4)	2.615(6)				
<i>Bond angles</i>							
O(5)–Mo(1)–N(1)	92.79(8)	N(3)–Mo(1)–O(7)	89.1(3)	N(2A)–Mo–O(4A)	89.1(2)	O(4A)–Mo–O(3)	176.9(1)
O(7)–Mo(1)–N(1)	95.85(8)	N(3)–Mo(1)–O(5)	90.6(3)	N(2A)–Mo–O(3)	91.0(2)	O(4A)–Mo–N(2A)	90.1(1)
O(3)–Mo(1)–N(1)	175.96(7)	O(7)–Mo(1)–N(1)	90.1(3)	O(4A)–Mo–N(1)	90.5(2)	O(3)–Mo–N(1)	90.5(1)
O(4)–Mo(2)–N(2)	174.60(8)	N(3)–Mo(1)–N(1)	175.1(3)	O(4A)–Mo–O(3)	176.9(2)	O(3)–Mo–N(2A)	89.5(1)
O(8)–Mo(2)–N(2)	92.16(8)	O(5)–Mo(1)–N(1)	89.9(3)	N(2A)–Mo–N(1)	175.3(2)	O(4A)–Mo–N(1)	89.6(1)
O(6)–Mo(2)–N(2)	96.34(8)	O(8)–Mo(2)–N(2)	90.1(3)	O(3)–Mo–N(1)	89.2(2)	N(2A)–Mo–N(1)	175.0(1)
		O(6)–Mo(2)–N(4)	89.8(3)				
		O(6)–Mo(2)–N(2)	90.5(3)				
		O(8)–Mo(2)–N(4)	89.3(3)				
		N(2)–Mo(2)–N(4)	174.9(3)				

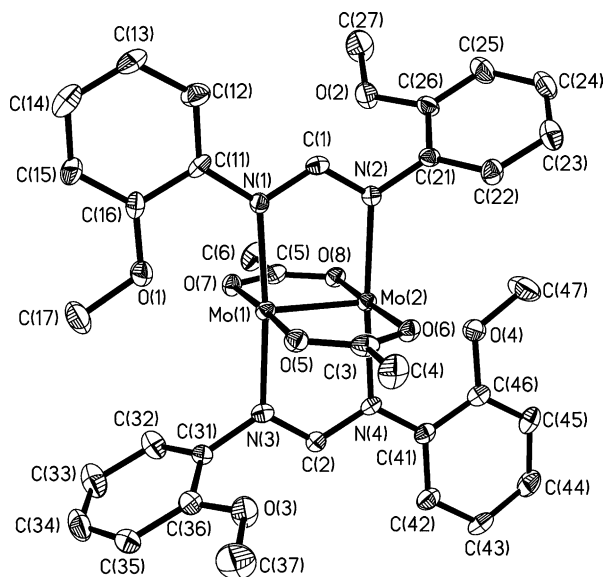


Fig. 2. ORTEP drawing for complex 2. Thermal ellipsoids shown at 50% probability level.

is in marked contrast to that found in the dichromium analogue $\text{Cr}_2(\text{O}_2\text{CCH}_3)_2(o\text{-DMophF})_2$ [18], in which the two chromium atoms are spanned by two *cis* bridging acetate ligands and two *cis* bridging *o*-DMophF[−] ligands. The *o*-DMophF[−] ligands of complexes 2–4 are arranged in the *s-cis, s-trans* conformation [15]. The OCH_3 group, which is in an orientation opposite to that of the methine hydrogen, forms a short $\text{Mo}\cdots\text{O}$ distance

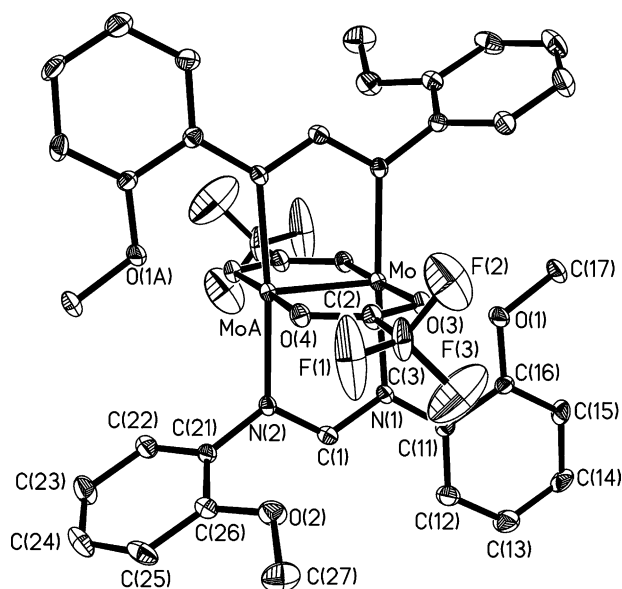


Fig. 3. ORTEP drawing for complex 3. Thermal ellipsoids shown at 50% probability level.

with one of the molybdenum atoms. Complexes 2–4 are of significance, because they are the first mixed ligands complexes which contain a pair of bridging acetate and a pair of bridging formamidinate ligands, although acetamidinate compound *trans*- $\text{Mo}_2(\text{O}_2\text{CCH}_3)_2(\text{DXy-lA})_2(\text{THF})_2$ 7a, and the benzamidinate compounds *trans*- $\text{Mo}_2(\text{O}_2\text{CCH}_3)_2[\mu\text{-}N,N'\text{-PhC(NSiMe}_3)_2]_2$ 7b and

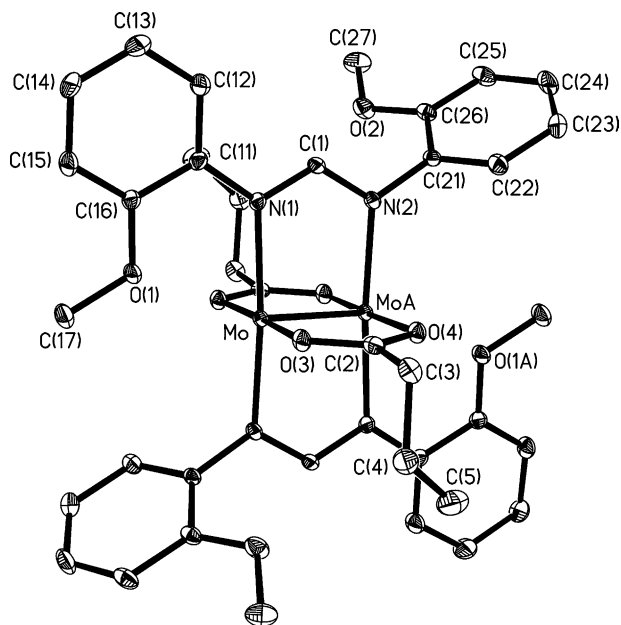


Fig. 4. ORTEP drawing for complex 4. Thermal ellipsoids shown at 50% probability level.

trans-Mo₂(O₂CPh)₂[μ-*N,N'*-PhC(NSiMe₃)₂]₂ [7c] have been reported.

Purple red crystals of **5** conform to the space group *P* $\bar{1}$ with one molecule in a unit cell. Fig. 5 shows the ORTEP diagram for **5**. Selected bond distances and angles for are listed in Table 3. The molecular structure consists of an asymmetric dimolybdenum unit [Mo–Mo = 2.1239 (6) Å] which are spanned by one bridging acetate ligand and one *o*-DMophF[–] ligand. A pair of chloride atoms and a pair of trimethylphosphine ligands occupy the remaining coordination sites. As a result, one

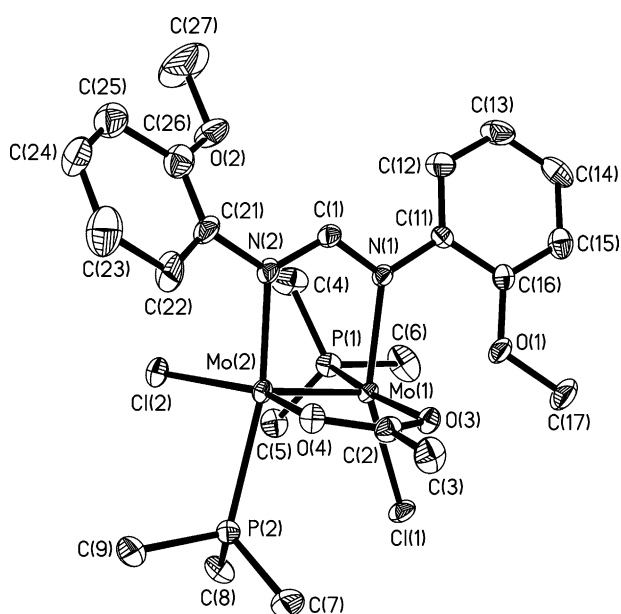


Fig. 5. ORTEP drawing for complex 5. Thermal ellipsoids shown at 50% probability level.

Table 3
Selected bond distances (Å) and angles (°) for **5**

Bond distances			
Mo(1)–Mo(2)	2.1239(6)	Mo(1)–N(1)	2.131(4)
Mo(1)–O(3)	2.163(3)	Mo(1)–Cl(1)	2.449(1)
Mo(1)–P(1)	2.507(2)	Mo(2)–O(4)	2.099(3)
Mo(2)–N(2)	2.125(5)	Mo(2)–Cl(2)	2.442(1)
Mo(2)–P(2)	2.537(2)	Mo(1)···O(1)	2.562(4)
Bond angles			
N(1)–Mo(1)–O(3)	92.7(2)	O(3)–Mo(1)–P(1)	169.03(10)
N(1)–Mo(1)–Cl(1)	153.84(12)	O(3)–Mo(1)–Cl(1)	89.80(10)
N(1)–Mo(1)–P(1)	87.24(11)	Cl(1)–Mo(1)–P(1)	85.53(5)
O(4)–Mo(2)–N(2)	91.6(2)	O(4)–Mo(2)–Cl(2)	151.34(11)
O(4)–Mo(2)–P(2)	85.46(11)	N(2)–Mo(2)–Cl(2)	90.34(13)
N(2)–Mo(2)–P(2)	166.45(12)	Cl(2)–Mo(2)–P(2)	85.98(5)

phosphine ligand and one chloride atom are *trans* to the acetate ligand and the others *trans* to the *o*-DMophF[–] ligand. The Mo–P and Mo–Cl bonds, 2.507 (2) and 2.442 (1) Å, respectively, that are *trans* to the acetate ligand have shorter bond distances than the corresponding bonds, 2.537 (2) and 2.449 (1) Å, respectively, that are *trans* to the *o*-DMophF[–] ligand, indicating that the acetate ligand has smaller *trans* influence than the *o*-DMophF[–] ligand. The Mo–O distances of complex **5**, 2.163 (3) and 2.099 (3) Å, which are *trans* to the trimethylphosphine ligand and chloride atom, respectively, are typical for complexes which are bridged by a single acetate ligand, i.e. Mo₂(OAc)[(PhN)₂CCH₃]₃ [19] 2.162 (5) Å, Mo₂(OAc)(ambt)₃(ambt = anion of 2-amino-4-methylbenzothiazole) [20], 2.16 (1) Å, Mo₂(O₂CCH₃)Cl₃(PMe₃)₃ [21], 2.10 (4) Å, (C₃N₂H₅)[Mo₂(OAc)[CH₃Ga(C₃N₂H₃)O]₄] [22], 2.102(8) Å and Mo₂(OAc)Cl₃(³η-tetraphos-2)(tetraphos-2 = P(CH₂CH₂PPh₂)₃) [23], 2.10(1) and 2.13(1) Å. The two different Mo–O distances in complex **5** indicate that trimethylphosphine ligand has a stronger *trans* influence than the chloride atom. In this complex, the *o*-DMophF[–] ligand is arranged in the *s-cis,s-trans* conformation and the OCH₃ group, which is in an orientation opposite to that of the methine hydrogen forms a short Mo···O distance with one of the molybdenum atoms.

4.2. Structural comparisons

A comparison of distances and angles observed for **1**–**5** is listed in Table 4. The Mo–Mo distances are typical for complexes containing a quadruple bond. In complexes, **1**, **2** and **5**, which contain the same acetate ligand, the one in which more acetate ligands are present the Mo–Mo distance is shorter. It seems that the acetate ligand has slight shortening effect over the *o*-DMophF[–] ligand. A comparison of complexes **2**, **3** and **4** shows that the one with the electronegative atom on the acetate ligand has the longer Mo–Mo distance. The length of

Table 4
Structural comparisons for complex 1–5

Compound	1	2	3	4	5
Mo–Mo (Å)	2.0933(3)	2.108(1)	2.133(2)	2.1088(6)	2.1239(6)
Mo···O (Å)	2.681(2)	2.600(7)	2.576(5)	2.602(2)	2.562(4)
∠ Mo–Mo···O (°)	2.667(2)	2.615(6)	159.5(1)	158.75(6)	154.0(1)
	152.97(5)	159.2(2)			
	154.33(5)	159.6(1)			

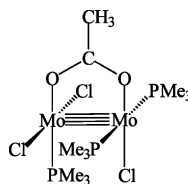
the alkyl chain has no influence on the distance of Mo–Mo bond. The distance of the Mo···O axial interaction is dependent on the strength of the Mo–Mo bond. The stronger is the Mo–Mo bond, the longer is the Mo···O distance. It is noted that although complex **1** has two Mo···O axial interactions, its Mo–Mo bond distance is similar to that of Mo₂(O₂CCH₃)₄, which is 2.0934 (8) Å. This is not unusual since it is well known that Mo–Mo quadruple bond is less sensitive to the axial interaction than the Cr–Cr quadruple bond [24].

4.3. NMR spectroscopy

The variable-temperature ¹H NMR spectra of complexes **1–4** show only a sharp singlet for the protons of OCH₃ groups, indicating that the solid state conformations of the *o*-HDMophF ligands in these complexes are not retained in CDCl₃ solution from room temperature to –60 °C. Similar situation was seen in the complexes Cr₂(*o*-DMophF)₄ [13] and Cr₂(O₂CCH₃)₂(*o*-DMophF)₂ [16]. However, due to the asymmetry of the molecules of complex **5**, two singlets for the two methoxy hydrogen atoms were observed, which appear at δ 3.23 and 3.40, respectively. The ³¹P{¹H} NMR spectrum of complex **5** also consists of two doublets centered at –3.58 and –8.37 ppm, respectively. The most striking information of this spectrum is the coupling constant of the 2 inequivalent phosphorus atoms, which is 15.2 Hz.

In a previous paper [23], we reported the structures and ³¹P{¹H} NMR spectra of two dimolybdenum complexes of the types Mo₂(OAc)Cl₃(³η-tetraphos-2) (tetraphos-2 = P(CH₂CH₂PPh₂)₃) and Mo₂(OAc)Cl₃(³η-etp) (etp = Ph₂PCH₂CH₂(Ph)CH₂CH₂PPh₂). An important aspect about the observed P–P coupling constants in these two complexes is the relative weighting of the contributions via the metal and via the ligand ‘backbone’. Assuming the Karplus-type angular dependence of the coupling constants to be minimal, and the coupling constant through backbone in the complex is similar to that in the free ligand, we concluded that the through metal–metal quadruple bonding coupling |³J_{P–Mo–Mo–P}| is about 20 ± 1 Hz. In complex **5**, no influence from the backbone has to be considered and, assuming the Karplus-type angular dependence of the coupling constants to be minimal, the |³J_{P–Mo–Mo–P}| is

15.2 Hz. To further verify this coupling constant, we have measured the ³¹P{¹H} NMR spectrum of Mo₂(OAc)Cl₃(PMe₃)₃ [21], shown as **I**, in which two monodentate phosphine ligands are positioned *cis* to the acetate ligand and one monodentate phosphine ligand *trans* to the acetate ligand. The ³¹P{¹H} NMR spectrum of this complex consists of one doublet and one triplet centered at –10.20 and –1.50 ppm, respectively, with a coupling constant of 16.3 Hz, which can be assigned to |³J_{P–Mo–Mo–P}|. Thus, we could probably conclude that, assuming the Karplus-type angular dependence of the coupling constants to be minimal, the |³J_{P–Mo–Mo–P}| is 16 ± 1 Hz. The 4 Hz difference as compared with 20 ± 1 Hz derived from Mo₂(OAc)Cl₃(³η-tetraphos-2) and Mo₂(OAc)Cl₃(³η-etp) is presumably due to the chelating and bridging bondings formed by the polydentate phosphine ligands to the metals.



I

In addition to the |³J_{P–Mo–Mo–P}| coupling constant, the |³J_{C–O–Mo–P}| and |³J_{C–N–Mo–P}| coupling constants derived in the ¹³C{¹H} NMR spectrum of complex **5** provide an opportunity to investigate the relative position of the monodentate phosphine ligand, i.e. *cis* or *trans* to the bridging acetate or formamidinate ligand. Fig. 6 shows the ¹³C{¹H} NMR spectrum of

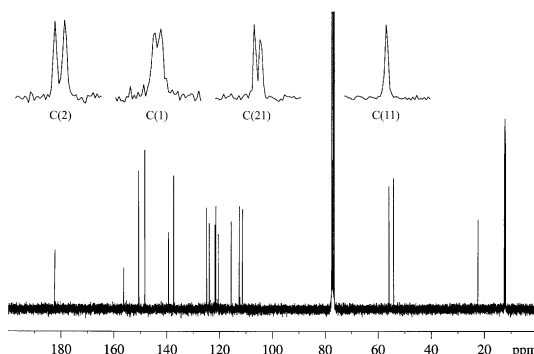


Fig. 6. ¹³C{¹H} NMR spectrum for complex **5**.

Table 5
Selected dihedral angle φ ($^\circ$) for **5**

P(1)–Mo(1)–N(1)–C(1)	101.9	P(2)–Mo(2)–N(2)–C(1)	170.0
P(1)–Mo(1)–O(3)–C(2)	1.8	P(2)–Mo(2)–O(4)–C(2)	98.8
P(1)–Mo(1)–N(1)–C(11)	104.2	P(2)–Mo(2)–N(2)–C(21)	173.1

complex **5** in CDCl_3 . The two peaks centered at 182.38 and 156.30 ppm can be assigned the central carbon atoms, C(1) and C(2), of the formamidinate and acetate ligands, respectively. A heteronuclear shift-correlated 2-D NMR spectrum for ^{13}C and ^1H nuclei shows that the peaks centered at 156.30 ppm is correlated with the methine hydrogen and can be assigned to C(1) of the formamidinate ligand. The peak at 182.38 ppm is then assigned to C(2). Both C(1) and C(2) atoms experience 3J coupling from two phosphorus atoms, but each peak only shows as a doublet with coupling constants of $|^3J_{\text{C(1)-P(1)}} + ^3J_{\text{C(1)-P(2)}}| = 2.2$ and $|^3J_{\text{C(2)-P(1)}} + ^3J_{\text{C(2)-P(2)}}| = 3.5$ Hz for C(1) and C(2), respectively. The two peaks centered at 139.34 and 137.36 ppm can be assigned either to C(11) or C(21) of the formamidinate ligand. Each of the carbon atoms experiences 3J coupling from one of the two phosphorus atoms and $|^3J_{\text{C(11)-P(1)}}|$ and $|^3J_{\text{C(21)-P(2)}}|$ are found to be 0 (due to the limit of the instrument resolution) and 2.1 Hz, respectively. The three-bond ^{13}C – ^{31}P coupling constants ($^3J_{\text{CP}}$) can be analyzed in terms of the generalized Karplus equation which relates the coupling constant to the dihedral angle (φ) in the four-atom fragment involved. The study generally resulted a Karplus curve showing maxima for J at $\varphi = 0$ and 180° , with the usual minimum at $\varphi = 90^\circ$ ($J \sim 0$ Hz) [25]. Table 5 lists some of the important dihedral angles for complex **5**. Based on the definite relation of Karplus equation, we can easily assign the peak at 137.37 ppm to C(11) which shows 0 Hz coupling constant, since the dihedral angle of O(1)–Mo(1)–N(1)–C(11) is close to 90° . We thus conclude that in the dimolybdenum complexes the phosphine ligand *cis* to the acetate or formamidinate ligands does not contribute to $^3J_{\text{C-P}}$ while the *trans* ligands contribute about 3 ± 1 Hz. The minimum φ of the $|^3J_{\text{C-P}}|$ Karplus curve for **5** and related complexes may appear at about 104° . Analysis of the $|^3J_{\text{C-P}}|$ coupling constant thus locates the position of the monodentate phosphine ligand for the dimolybdenum complexes with bridging acetate or similar ligands. To further verify this proposition, we have measured the $^{13}\text{C}\{^1\text{H}\}$ NMR spectrum of $\text{Mo}_2(\text{OAc})\text{Cl}_3(\text{PMe}_3)_3$, which shows only as a doublet for the central carbon atom of the acetate ligand, with a $|^3J_{\text{C-P}}|$ coupling constant of 3.5 Hz.

5. Concluding remarks

Five complexes, which contain *o*-DMophF[−] ligands and one, two or three acetate ligands have been structurally characterized. The Mo–Mo bond length is dependent on the number of the acetate ligands and on the electronegativity of the substituent on the acetate ligand. Two different conformations, *s-trans,s-trans* and *s-cis,s-trans*, are seen for the *o*-HDMophF[−] ligand. In complexes **1–5**, which conformation to take is dependent on the number of the methoxyl group each ligand has to provide to accommodate the two axial sites of the dimolybdenum unit, although the Mo–Mo bond length is not sensitive to such axial interactions. Complex **5** provides an opportunity to study the through metal–metal quadruple bonding coupling $|^3J_{\text{P-Mo-Mo-P}}|$ without considering the ligand ‘backbone’ contribution and the result is 16 ± 1 Hz. The position of the monodentate phosphine ligand can be determined by evaluating the $|^3J_{\text{C-P}}|$ coupling constant. Complexes **1–4** can be envisaged as the intermediates of the stepwise decarboxylation of $\text{Mo}_2(\text{O}_2\text{CR})_4$ to form $\text{Mo}_2(\text{form})_4$.

6. Supplementary material

Crystallographic data (excluding structure factors) for the structures in this paper have been deposited with the Cambridge Crystallographic Data Centre as supplementary publication numbers CCDC 178806–178810. Copies of the data can be obtained, free of charge, on application to CCDC, 12 Union Road, Cambridge CB2 1EZ, UK (fax: +44-1223-336 033; or e-mail: deposit@ccdc.cam.ac.uk).

Acknowledgements

We wish to thank the National Science Council of the Republic of China for support.

References

- [1] C. Lin, J.D. Protasiewicz, T. Ren, *Inorg. Chem.* 35 (1996) 7455.
- [2] C. Lin, J.D. Protasiewicz, E.T. Smith, T. Ren, *Inorg. Chem.* 35 (1996) 6422.
- [3] T. Ren, C. Lin, P. Amalberti, D. Macikenas, J.D. Protasiewicz, J.C. Baum, T.L. Gibson, *Inorg. Chem. Commun.* 1 (1998) 23.
- [4] M.H. Chisholm, F.A. Cotton, L.M. Daniels, K. Folting, J.C. Huffman, S.S. Iyer, C. Lin, A.M. Macintosh, C.A. Murillo, *J. Chem. Soc., Dalton Trans.* (1999) 13872.
- [5] R. Clérac, F.A. Cotton, K.R. Dunbar, C.A. Murillo, X. Wang, *Inorg. Chem.* 40 (2001) 420.
- [6] T. Ren, *Coord. Chem. Rev.* 175 (1998) 43.
- [7] (a) F.A. Cotton, W.H. Ilsley, W. Kaim, *Inorg. Chem.* 20 (1981) 930;
(b) G. Zou, T. Ren, *Inorg. Chem. Acta* 304 (2000) 305;

- (c) A. Zinn, F. Weller, K. Dehnick, *Z. Anorg. Allg. Chem.* 594 (1991) 106;
- (d) F.A. Cotton, L.M. Daniels, C. Lin, C.A. Murillo, *J. Am. Chem. Soc.* 121 (1999) 4538.
- [8] A.B. Brignole, F.A. Cotton, *Inorg. Synth.* 13 (1972) 81.
- [9] F.A. Cotton, J.G. Norman, *J. Coord. Chem.* 1 (1971) 161.
- [10] T.A. Stephenson, E. Bannister, G. Wilkinson, *Inorg. Synth.* (1964) 2538.
- [11] S.J. Archibald, N.W. Alcock, D.H. Busch, D.R. Whitcomb, *Inorg. Chem.* 38 (1999) 5571.
- [12] G.M. Sheldrick, *SHELXTL*, Release 5.03, Siemens Analytical X-ray Instruments Inc., Karlsruhe, Germany, 1993.
- [13] F.A. Cotton, L.M. Daniels, C.A. Murillo, P.J. Schooler, *Chem. Soc., Dalton Trans.* (2000) 2007.
- [14] T. Ren, V. Desilva, G. Zou, C. Lin, L.M. Daniels, C.F. Campana, J.C. Alvarez, *Inorg. Chem. Commun.* 2 (1999) 301.
- [15] S. Radak, Y. Ni, G. Xu, K.L. Shaffer, T. Ren, *Inorg. Chim. Acta* 321 (2001) 200.
- [16] D.M. Baird, P.E. Fanwick, T. Barwick, *Inorg. Chem.* 24 (1985) 3753.
- [17] D.M. Baird, K.Y. Shih, J.H. Welch, R.D. Bereman, *Polyhedron* 8 (1989) 2359.
- [18] F.A. Cotton, L.M. Daniels, C.A. Murillo, P. Schooler, *J. Chem. Soc., Dalton Trans.* (2000) 2001.
- [19] F.A. Cotton, W.H. Ilsley, W. Kaim, *Inorg. Chem.* 20 (1981) 930.
- [20] F.A. Cotton, W.H. Ilsley, *Inorg. Chem.* 10 (1981) 572.
- [21] P.A. Bates, A.J. Nielson, J.M. Waters, *Polyhedron* 6 (1987) 2111.
- [22] K.R. Breakell, S.J. Rettig, A. Storr, J. Trotter, *Can. J. Chem.* 61 (1983) 1659.
- [23] C.-T. Lee, S.-F. Chiang, C.-T. Chen, J.-D. Chen, C.-D. Hsiao, *Inorg. Chem.* 35 (1996) 2930.
- [24] F.A. Cotton, R.A. Walton, *Multiple Bonds between Metal Atoms*, 2nd ed., Oxford University Press, London, 1993.
- [25] L.D. Quin, Stereospecificity in ^{31}P -element couplings: phosphorus–carbon coupling, in: J.G. Verkade, L.D. Quin (Eds.), *Phosphorus-31 NMR Spectroscopy in Stereochemical Analysis*, VCH Publishers, Deerfield Beach, FL, 1987.